Available online at www.sciencedirect.com
SCIENCE DIRECT®
Journal of Solid State Chemistry 172 (2003) 389–395
JOURNAL OF SOLID STATE CHEMISTRY
http://elsevier.com/locate/jssc

Evidence for a monoclinic distortion in the ferroelectric Aurivillius phase $Bi_3LaTi_3O_{12}$

M.-W. Chu, M.T. Caldes, Y. Piffard,* A.-M. Marie, E. Gautier, O. Joubert, M. Ganne, and L. Brohan

Institut des Matériaux Jean ROUXEL, UMR CNRS-Université de Nantes no. 6502 2, rue de la Houssinière, BP 32229-44322 Nantes Cedex 3, France

Received 16 July 2002; received in revised form 15 November 2002; accepted 24 November 2002

Abstract

An alternative chemical approach was used to prepare the ferroelectric Aurivillius phase $Bi_3LaTi_3O_{12}$ (BLT1.00) at low temperature (450°C) leading to well-crystallized compounds at 750°C. The existence of 90°-oriented twin domains, characteristic of a ferroelectric state, was revealed in selected area electron diffraction and microdiffraction studies. Though the 3D reconstruction of the reciprocal lattice enables to propose the non-centrosymmetrical orthorhombic space group (SG) *B*2*cm*, a further convergent-beam electron diffraction study was undertaken in order to ascertain the symmetry. The monoclinic symmetry was clearly identified. BLT1.00 crystallizes in the polar SG *B*1*c*1 (no. 7, non-standard setting of *P*1*c*1) instead of *I*4/*mmm*, as previously reported.

1. Introduction

The ferroelectric random access memories (FRAM) have attracted much attention during the last decades due to their low-power requirements, fast access speed, and low cost [1–4]. Early works concerning the search of FRAM candidate materials were devoted to the $Pb(Zr_xTi_{1-x})O_3$ (PZT) thin films for their large remanent polarization and low processing temperature, but PZT suffers severe "fatigue" problems on metal electrodes (Pt) after repeated bipolar switching [3,4]. Recently, the two-layer ($n = 2$) ferroelectric Aurivillius phase $SrBi_2Ta_2O_9$ (SBT) [3] and the three-layer ($n = 3$) $Bi_{3.25}La_{0.75}Ti_3O_{12}$ (BLT0.75) [4] have been used as substituting materials for PZT due to their fatigue-free characteristics on Pt electrodes.

The structure of Aurivillius phases can be described as the intergrowth of fluorite-like $(Bi_2O_2)^{2+}$ units and perovskite-like $(A_{n-1}B_nO_{3n+1})^{2-}$ slabs, where $n = 2$, 3, 4, and 5 [5]. The 12-fold perovskite A sites can be occupied by cations like Ba^{2+}, Ca^{2+}, Sr^{2+}, Bi^{3+}, and the rare-earth cations, and the six-fold B sites by cations like Ti^{4+}, Ta^{5+}, Nb^{5+}, and W^{6+}, leading to BO_6 octahedra [6]. The idealized structure (space group (SG) *I*4/*mmm*; $a_{tet} \approx 3.86$ Å and $c_{tet} \approx 32.8$ Å) of the $n = 3$ Aurivillius compound $Bi_4Ti_3O_{12}$ (BTO) is shown in Fig. 1 [5].

The actual crystal structure of the prototype BTO has been determined by Rae et al. [7] from single-crystal X-ray diffraction (XRD) data. It was described as a commensurate modulation ($q = b^*$) of an orthorhombic average structure (SG *Fmmm* no. 69; $a_{orth} \approx b_{orth} \sim a_{tet}\sqrt{2}$ and $c_{orth} = c_{tet}$) leading to the monoclinic SG *B*1*a*1 (no. 7, non-standard setting of *P*1*c*1) with $a_{mon} = 5.450(1)$ Å, $b_{mon} = 5.4059(6)$ Å, $c_{mon} = 32.832(3)$ Å, and $\beta = 90.00°$ (the non-conventional B centering is used for ease of comparison with the parent *I*4/*mmm* prototype and the *a*- and *b*-axis corresponding to the diagonals $a_{tet} \pm b_{tet}$ of the parent structure).

Concerning the three-layer lanthanum bismuth titanates, the crystal structure of $Bi_{4-x}La_xTi_3O_{12}$ members with $x = 1$ and 2 was analyzed from a combination of X-ray and neutron powder diffraction data, using the centrosymmetrical SG *I*4/*mmm*, no. 139 [6]. However, in a lately study of the $Bi_{4-x}La_xTi_3O_{12}$ solid solution ($0 \leqslant x \leqslant 1.00$) [8], in the form of thin films, it has been demonstrated that $Bi_3LaTi_3O_{12}$ (BLT1.00) shows a saturated hysteresis loop with a remanent polarization of 4.5 μC/cm^2. Therefore, the actual SG for this

*Corresponding author. Lab de Chimie des Solides, Institut des Matériaux, 2 rue de la Houssinière BP 32229, 44322 Nantes Cedex 03, France. Fax: +33-2-40-37-39-95.
E-mail address: piffard@cnrs-imn.fr (Y. Piffard).

0022-4596/03/$ - see front matter © 2003 Elsevier Science (USA). All rights reserved.
doi:10.1016/S0022-4596(03)00015-X

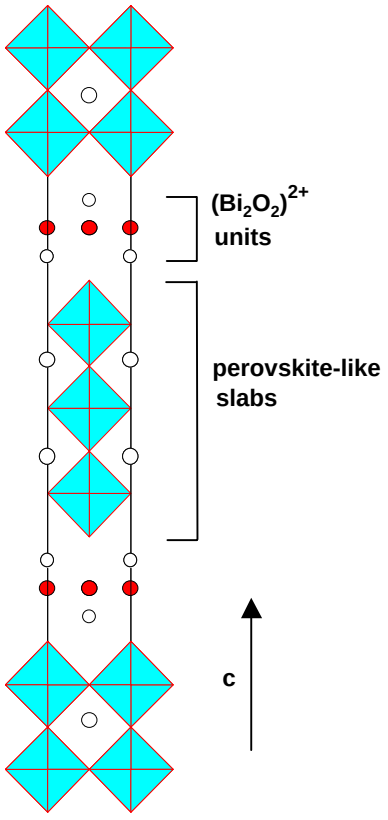

Fig. 1. [100] view of the idealized ($I4/mmm$) structure of the $n = 3$ Aurivillius phase $Bi_4Ti_3O_{12}$.

compound cannot be $I4/mmm$. In order to resolve this ambiguity, a microstructural study of BLT1.00 has been performed.

In this paper, an alternative chemical approach to synthesize $Bi_3LaTi_3O_{12}$ and a comprehensive electron diffraction study using several techniques (selected area electron diffraction (SAED), microdiffraction and convergent-beam electron diffraction (CBED)) are reported.

2. Experimental

The Pechini method [9] was used to synthesize $Bi_3LaTi_3O_{12}$ and the detailed sample preparation is described in the next section.

The phase purity of powder samples was controlled by XRD with the use of a Siemens D5000 diffractometer (Cu$K\alpha$ radiation) and cell parameters were refined by full pattern matching using RIETICA software [10].

SAED, microdiffraction, and CBED studies were performed on a Philips CM30 electron microscope operating at 300 kV. With this microscope, the sample composition was verified on many crystals by energy dispersive X-ray analysis (EDX) (Link System OXFORD analyzer).

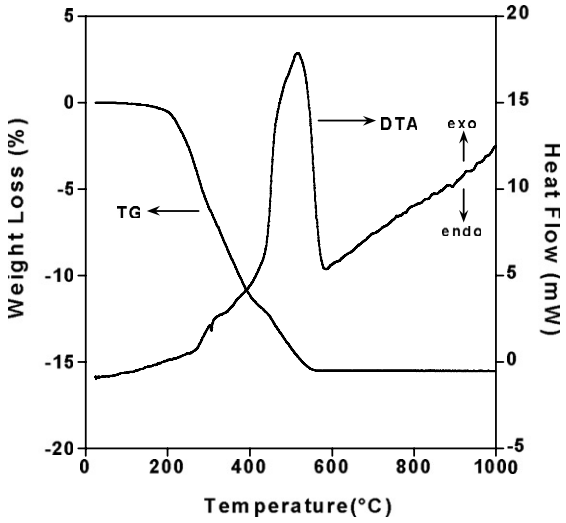

Fig. 2. TG/DTA curves of the polymer precursor.

Thermogravimetry (TG) and differential thermal analysis (DTA) were performed on a Setaram Type 92 microbalance. The experiments were carried out in air, up to 1000°C, at a heating rate of 10°C/min.

3. Results and discussion

3.1. Synthesis and XRD analyses

Due to the volatility of bismuth, a low-temperature approach was preferred in order to control the sample stoichiometry.

$Bi(NO_3)_3 \cdot 5H_2O$ (99.99%, Aldrich), $La(NO_3)_3 \cdot 6H_2O$ (99.99%, Riedel-de Haën), $TiC_{10}H_{14}O_5$ (98%, Merck), citric acid (CA: 99%, Aldrich) and ethylene glycol (EG: 99%, Aldrich) were taken as the starting chemicals, and methanol (MeOH: 98%, Merck) was used as solvent. The optimized molar ratio of $TiC_{10}H_{14}O_5$:CA:EG and concentration of the CA solution in MeOH were kept at 1:10:40 and 1 M, respectively. 0.1 mol of $TiC_{10}H_{14}O_5$ was first dissolved in the CA/MeOH solution. Then, 0.1 mol of bismuth nitrate and 0.033 mol of lanthanum nitrate were separately added into this solution along with 4 mol of EG and 1.5×10^{-3} mol of HNO_3. The yellowish transparent mixture was stirred at 100°C for $\frac{1}{2}$ h leading to the metal–citrate complexes, which were then polymerized in a microwave oven. The as-prepared polymer was fired at 400°C for 2 h to burn out most of the organic species, and this "powder precursor" was ground and pressed into pellets prior to the final heat treatment at various temperatures in air.

Thermal analysis data, shown in Fig. 2, were recorded in order to analyze the thermal behavior of the precursor. The TG curve, shows that a weight loss occurs in two steps between 200°C and 550°C. Such

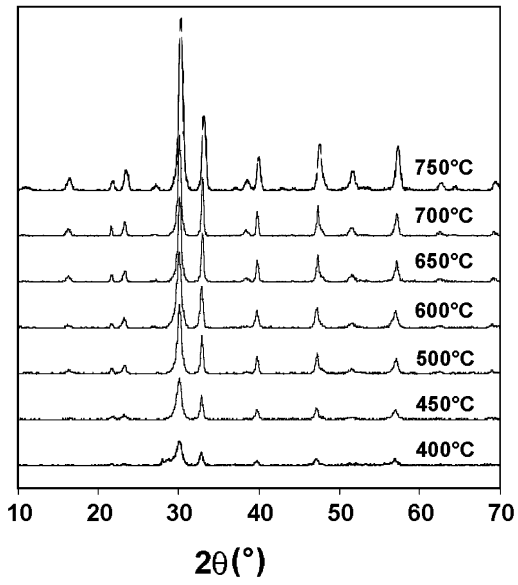

Fig. 3. XRD patterns of the powder precursor heated for 2 h at temperatures ranging from 450°C to 750°C.

steps are also characterized by two exothermic peaks at ~320°C and ~520°C on the DTA curve. From 550°C to 1000°C a plateau region is observed on the TG curve and no thermal event is found on the DTA curve. These results suggest that all nitrates and organic species are decomposed below 550°C and that there is no loss of bismuth up to 1000°C (within the detection limits of the apparatus).

Pellets of the "powder precursor" were heated in air at various temperatures ranging from 450°C to 750°C for 2 h and then ground into powders for further XRD analyses. The corresponding patterns are displayed in Fig. 3 along with that of the "powder precursor" (heated at 400°C). Remarkably, the "powder precursor" appears as partially crystallized although the weight loss is far from being complete. Its pattern already shows the most intense lines of the single-phase compound. Upon a further heating at 450°C for 2 h, a rather well crystallized compound is obtained. Its TG analysis does not show any weight loss, thus indicating that the steady mass observed at 550°C in Fig. 2 can be reached upon this new thermal treatment at 450°C.

For the structural characterization, a pellet of the "powder precursor" was heated at 750°C for 24 h. EDX elemental analyses were performed on many crystals of this sample. The results are in good agreement with the nominal composition and attest that the sample is homogeneous. Attempts were then made to refine tetragonal (SG $I4/mmm$ with $a \approx 3.83$ Å and $c \approx 31.91$ Å) or orthorhombic (SG $Fmmm$ with $a \approx b \approx 5.416$ Å and $c \approx 31.91$ Å) cell parameters from the XRD pattern. They were both leaving at least five rather weak reflections unindexed at $2\theta(^\circ) \approx 19.6$, 38.7, 48.3, 51.8, and 62.8 (Fig. 4), whereas such reflections

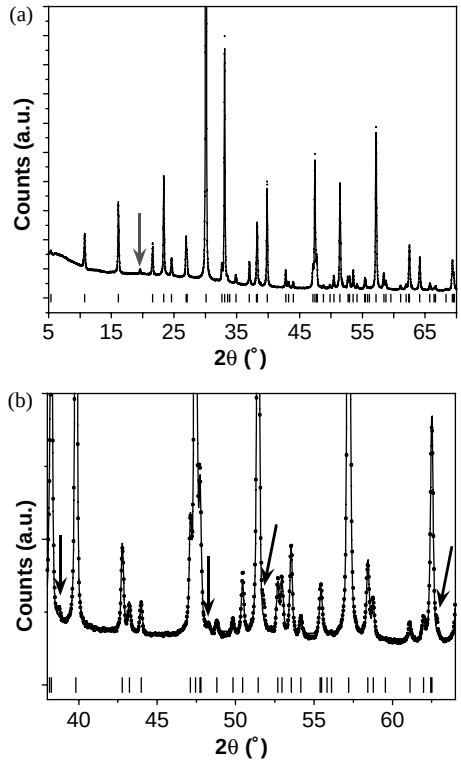

Fig. 4. XRD pattern of $Bi_3LaTi_3O_{12}$ prepared from the powder precursor at 750°C for 24 h (a) and expanded part (b). Reflections marked by arrows cannot be indexed with SG $I4/mmm$ and $Fmmm$ (see text).

were perfectly taken into account when a B (or A) centered orthorhombic cell was considered, leading to $a = 5.4164(2)$ Å, $b = 5.4157(3)$ Å, $c = 32.9133(2)$ Å.

From the results described above, it can be seen that the Pechini method enables to prepare the BLT1.00 phase at lower temperature than by conventional solid state reactions and therefore to achieve an easier control of the homogeneity and stoichiometry.

3.2. Electron diffraction studies

The XRD study suggests that, as in the case of BTO [7], BLT1.0 likely exhibits a small displacive perturbation away from an $I4/mmm$ parent structure (This latter one should correspond to the crystal structure of the paraelectric phase, i.e. above the so-called Curie temperature). In order to confirm this, the SG identification was undertaken. First, the existence conditions were inferred from SAED and microdiffraction experiments. Then, although no deviation from metric orthorhombic symmetry could be observed, the CBED technique was used to identify the 3D point group.

3.2.1. SAED and microdiffraction studies

Fig. 5 shows SAED patterns of the BLT1.00 compound along two zone axes: [001] (Fig. 5a) and [110]

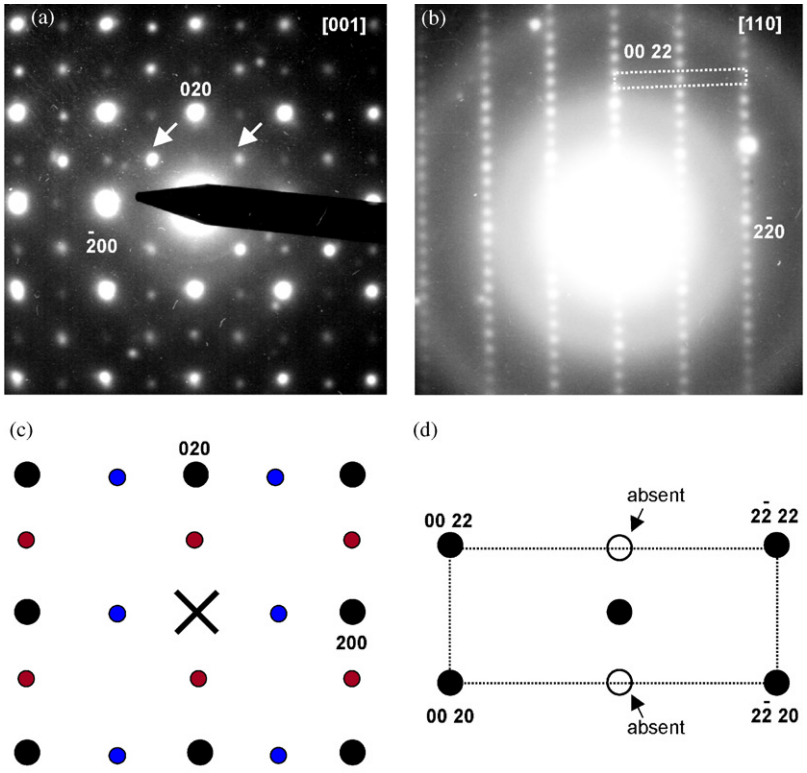

Fig. 5. SAED and schematized patterns of $Bi_3LaTi_3O_{12}$ along the [001] (a and c), and [110] (b and d) zone axes.

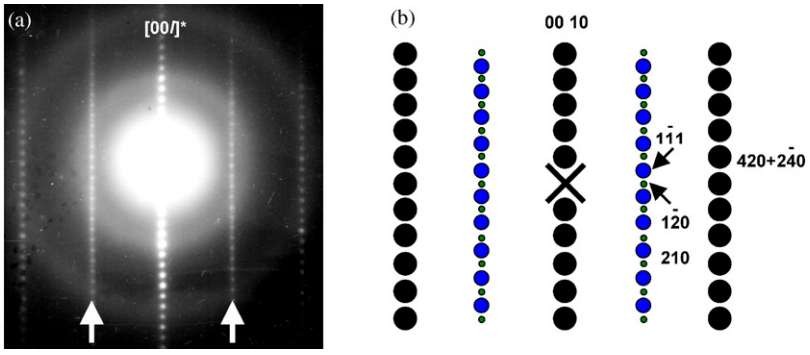

Fig. 6. SAED (a) and schematized (b) patterns corresponding to the superimposition of [$\bar{1}$20] and [210] zone axes.

(Fig. 5b). As schematized in Fig. 5d one can note that $\bar{h}h0$ and $h\bar{h}0$ reflections with odd h values are not observed in Fig. 5b, whereas they appear in Fig. 5a (as indicated by white arrows). In fact, all the reflections with h and k both odd in the $(hk0)^*$ plane arise from the first-order Laüe zone (FOLZ, i.e. $l = 1$), which means that $h\,k\,0$ reflections with h and k both odd do not exist. Therefore, the $(hk0)^*$ plane appears as a square array of intense reflections $(h, k = 2n)$ with supplementary less intense reflections in the middle of each side of these squares, but nothing in their center (Fig. 5c). This kind of pattern reveals the existence of 90°-oriented twin domains in the crystals. Such domains must be smaller than the typical probe size of the SAED technique, i.e. 500 nm. Their observation by HREM is presently being undertaken and images will be published in a forthcoming paper.

As a consequence of 90°-oriented twin domains, the SAED patterns containing the $[00l]^*$ row appear in all cases as a superimposition of $[hk0]$ and $[\bar{k}h0]$ zone axis patterns (ZAPs), which are nearly perpendicular ($a \approx b$). This is illustrated in Fig. 6a for $h = \bar{1}$ and $k = 2$. Rows of reflections parallel to $[00l]^*$ (on the right-hand side of Fig. 6a) correspond to $21l + 1\bar{2}l$ reflections for the first row, and $42l + 2\bar{4}l$ reflections for the second row (Fig. 6b). In this latter row, reflections are observed for even l indices only, which reveals the existence condition $h + l = 2n$ for $h\,k\,l$ reflections, indicating a B centering. In agreement with this, $0\,0\,l$ reflections are observed for even l indices only, and reflections with odd

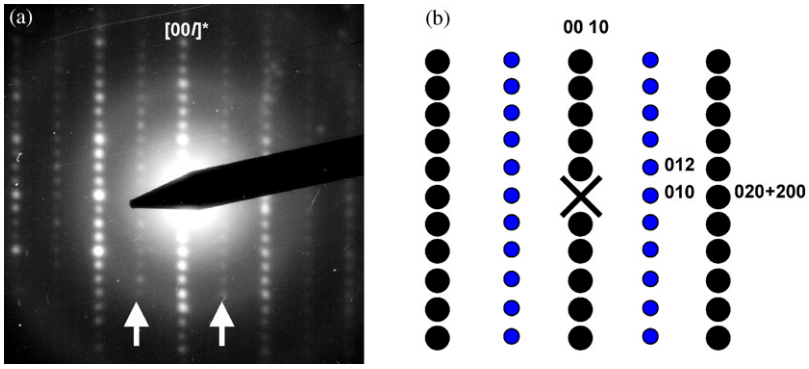

Fig. 7. SAED (a) and schematized (b) patterns corresponding to the superimposition of [100] and [010] zone axes.

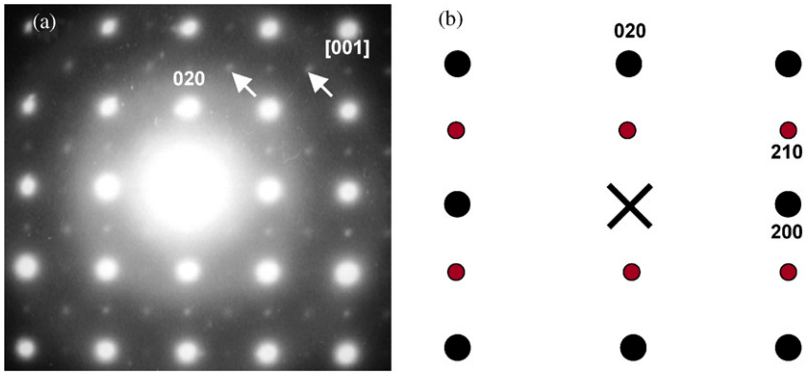

Fig. 8. Microdiffraction (a) and schematized (b) pattern of the [001] zone axis (spot size: 50 nm).

and even l indices appear in the row of $21l + 1\bar{2}l$ reflections because the B centering implies $l = 2n$ for $21l$ reflections and $l \neq 2n$ for $21l$ reflections. The pattern of Fig. 7a could correspond to a [100] ZAP because within $[0kl]^*$ rows with $k \neq 2n$ (indicated by white arrows), reflections only appear for $l = 2n$ in agreement with a B centered lattice (Fig. 7b). In the case of a [010] ZAP, reflections within $[h0l]^*$ rows with $(h \neq 2n)$ should either be absent (implying a c glide plane perpendicular to [010]), or appear for $l \neq 2n$ only, due to the B type centering. However, though many attempts were made, this [010] ZAP has never been observed in SAED experiments, whereas patterns similar to that of Fig. 7a have been observed very frequently. As the structural arrangement is almost the same along a- and b-axis, preferential orientation for $(0kl)$ with respect to $(h0l)$ is very unlikely. Therefore, this failure to observe a [010] ZAP is likely a consequence of domains leading to superimposed [100] and [010] ZAPs. In the corresponding patterns, the first row of reflections parallel to $[00l]^*$ (as on the right-hand side of Fig. 7a) would correspond to $0\,1\,l + 1\,0\,l$ reflections. At this level, it must be mentioned that in all patterns similar to that of Fig. 7, reflections only appear for $l = 2n$ within the first row of reflections parallel to $[00l]^*$. Therefore, assuming that one is dealing with domains, this result indicates that $1\,0\,l$ reflections do not exist, i.e. the existence condition $h\,0\,l,\ h, l = 2n$ is fulfilled.

In the hope of extracting structural information from a single domain, a microdiffraction study was performed with a spot size of 50 nm. The [001] ZAP is shown in Fig. 8a and schematized in Fig. 8b. Analogous to the SAED pattern of Fig. 5a, weak reflections with h and k both odd in the $(hk0)^*$ plane (indicated by white arrows) arise from the FOLZ. In addition, though weak, some $h\,k\,0$ $(h = 2n,\ k \neq 2n)$ reflections are observed, while those with $(h \neq 2n,\ k = 2n)$ are no longer observed as schematized in Fig. 8b, thus confirming that this particular pattern corresponds to a single domain. Meanwhile, though the spot size was reduced down to 12 nm, all attempts to identify a [010] ZAP failed. However, the two patterns of Fig. 9, taken from two different parts of the same crystal while keeping the same orientation, are of particular interest. They show that the intensity of reflections within the first row parallel to $[00l]^*$ (indicated by white arrows) decreases significantly when going from Fig. 9a and b, whereas the intensity of reflections within the second row (as well as that of $0\,0\,l$ reflections) remains the same. This result means that, though several domains are still present in this crystal, their relative proportion is not the same

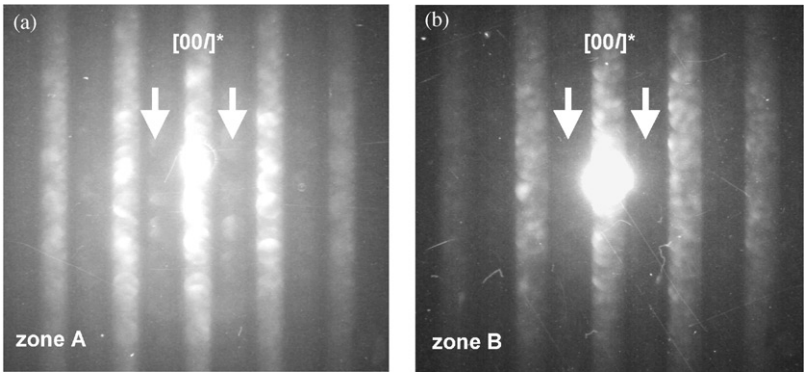

Fig. 9. Electron diffraction patterns from two parts ((a) and (b)) of a crystal in the same orientation (spot size: 12 nm).

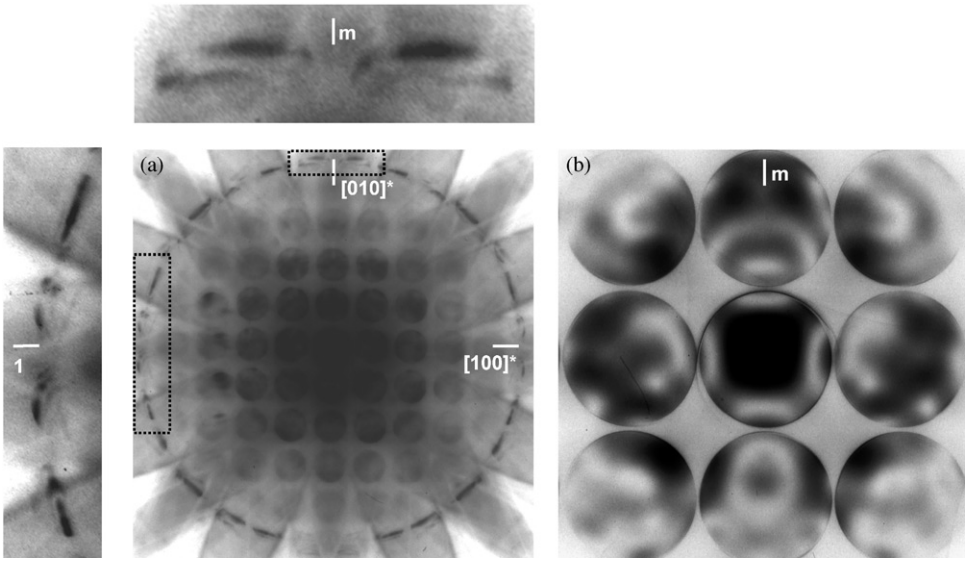

Fig. 10. CBED patterns of $Bi_3LaTi_3O_{12}$ along the [001] zone axis : Whole pattern (a) (details delimited by doted rectangles are displayed on an expanded scale), BF (b).

in the two parts, and Fig. 9b predominantly appears as a [010] ZAP.

In summary, the SAED and microdiffraction studies leads to existence conditions ($h\,k\,l$: $h+l=2n$; $0\,k\,l$: $l=2n$; $h\,0\,l$: $h,l=2n$; $h\,k\,0$: $h=2n$) which enables to propose the non-centrosymmetrical orthorhombic SG $B2cm$ (no. 39, non-standard setting of $Abm2$). However, since it has been demonstrated that the prototype compound BTO crystallizes in the monoclinic system (SG $B1c1$) in a cell of dimensions $a=5.450(1)$ Å, $b=5.4059(6)$ Å, $c=32.832(3)$ Å, and $\beta=90.00^{\circ}$, the BLT1.00 phase was further investigated with the use of the CBED technique in order to ascertain the symmetry.

3.3. CBED study

A method proposed by Buxton et al. [11] was used to determine the 3D point group. The whole pattern (WP) of BLT1.00 taken from [001] incidence is shown in Fig. 10a. It contains many Kikuchi lines and reflexions belonging to the FOLZ which form a ring around the zero-order Laüe zone. If the SG is $B2cm$ as inferred from SAED and microdiffraction studies, i.e. if the point group is $2mm$ (non-standard setting of $mm2$), the *diffraction group* [12] of the [001] zone axis pattern should be $2mm$ (Table 1). Taking into consideration the positions of diffracted disks and the dynamical diffraction contrast within such disks, it appears that the mirror plane does not exist along $[100]^*$, whereas it is observed only along the $[010]^*$ direction (see details of Fig. 10a on an expanded scale). Therefore, the WP symmetry is m. It can be seen (Fig. 10b) that the bright-field (BF) symmetry is also m. From Table 1, the 3D point group of BLT1.00 thus refers to either $2/m$ or m. Considering the ferroelectric behavior of this phase [8] the 3D point group must be m. Consequently, on account of the existence conditions inferred from the SAED and microdiffraction studies, the SG is identified as $B1c1$ (no. 7, non-standard setting of $P1c1$).

Table 1
3D point group and CBED pattern symmetries [11,12]

System	3D point group	Whole pattern	Bright field	Diffraction group
Monoclinic	m	m	m	m
	$2/m$	m	m	$2RmmR$ } $[U0W]$ZAP
Orthorhombic	$mm2$	$2mm$	$2mm$	$2mm \leftarrow$ [001]ZAP

4. Conclusion

The ferroelectric Aurivillius phase $Bi_3LaTi_3O_{12}$ can be prepared at 450°C via the Pechini method and it is well crystallized at 750°C. This chemical approach enables an easier control of the homogeneity and stoichiometry.

The selected area electron diffraction study of $Bi_3LaTi_3O_{12}$ crystals reveals the existence of 90°-oriented twin domains. Such domains, also observed in a subsequent microdiffraction study, are very small in size (less than 12 nm). The 3D reconstruction of the reciprocal lattice enables to identify the non-centrosymmetrical orthorhombic space group $B2cm$. However, the convergent-beam electron diffraction study of [001] zone finally indicates that $Bi_3LaTi_3O_{12}$ crystallizes in SG $B1c1$ (no. 7) of the monoclinic system.

References

[1] N.W. Schubring, R.A. Dork, J.P. Nolte, J. Appl. Phys. 38 (1967) 1671.
[2] J.F. Scott, C. A-Paz de Araujo, Science 246 (1989) 1400.
[3] C. A-Paz de Araujo, J.D. Cuchiaro, L.D. McMillan, M.C. Scott, J.F. Scott, Nature 374 (1995) 627.
[4] B.H. Park, B.S. Kang, S.D. Bu, T.W. Noh, J. Lee, W. Jo, Nature 401 (1999) 682.
[5] B. Aurivillius, Ark. Kemi 1 (1949) 499.
[6] C.H. Hervoches, P. Lightfoot, J. Solid State Chem. 153 (2000) 66.
[7] A.D. Rae, J.G. Thompson, R.L. Withers, A.C. Willis, Acta Crystallogr. B 46 (1990) 474.
[8] D. Wu, A. Li, T. Zhu, Z. Li, Z. Liu, N. Ming, J. Mater. Res. 16 (2001) 1325.
[9] P. Pechini, US Patent No. 3,330,697, July 11, 1967.
[10] B. Hunter, LHPM-Rietica Rietveld, ANSTO, Australia, 2000.
[11] B.F. Buxton, J.A. Eades, J.W. Steeds, G.M. Rackham, Philos. Trans. R. Soc. 281 (1976) 181.
[12] D.B. Williams, C.B. Carter, in: Transmission Electron Microscopy, Vol. II, Plenum Press, New York, 1996, pp. 331–334.